QPI for Prostate Cancer Diagnosis: Quantitative Separation of Gleason Grades 3 and 4

Shamira Sridharan[1], Virgilia Macias[2], Krishnarao Tangella[3], Andre Kajdacsy-Balla[2], and Gabriel Popescu[*4]

[1]Quantitative Light Imaging Laboratory, Bioengineering Department, Beckman Institute of Advanced Science and Technology, University of Illinois at Urbana-Champaign, Urbana, IL 61801, USA; [2]University of Illinois at Chicago, Department of Pathology, Chicago, Illinois 60612, USA; [3]Christie Clinic and University of Illinois at Urbana-Champaign, Department of Pathology 1400 West Park Street, Urbana, Illinois 61801, USA. [4]Quantitative Light Imaging Laboratory, Department of Electrical and Computer Engineering, Beckman Institute of Advanced Science and Technology, University of Illinois at Urbana-Champaign, Urbana, IL 61801, USA.

*gpopescu@illinois.edu; phone: 217-333-4840; light.ece.illinois.edu

ABSTRACT

1 in 7 men receive a diagnosis of prostate cancer in their lifetime. The aggressiveness of the treatment plan adopted by the patient is strongly influenced by Gleason grade. Gleason grade is determined by the pathologist based on the level of glandular formation and complexity seen in the patient's biopsy. However, studies have shown that the disagreement rate between pathologists on Gleason grades 3 and 4 is high and this affects treatment options. We used quantitative phase imaging to develop an objective method for Gleason grading. Using the glandular solidity, which is the ratio of the area of the gland to a convex hull fit around it, and anisotropy of light scattered from the stroma immediately adjoining the gland, we were able to quantitatively separate Gleason grades 3 and 4 with 81% accuracy in 43 cases marked as difficult by pathologists.

Keywords: prostate cancer, cancer diagnosis, Gleason grading, quantitative phase imaging, spatial light interference microscopy, microscopy, interferometry, label-free imaging, tissue microarray

1. INTRODUCTION

98.9% of men diagnosed with prostate cancer between the years 2004 – 2010 survived 5 years or longer [1]. When the data is further categorized based on disease stage at diagnosis, 80.7% of the cancers were diagnosed at the local stage, during which the 5 year survival rate is 100% [1]. However, the 5-year survival rate for individuals with distant metastasis of prostate cancer is 28%. Hence diagnosis of prostate cancer at an early stage, when it has a higher chance for cure, is critical for patient survival. However, various studies have shown that not all prostate cancers diagnosed at an early stage require intervention [2,3]. A particularly compelling argument towards this end was provided from a study by Porter et. al. that showed that 1.2 million new cases of prostate cancer would be diagnosed if all men between the ages of 62-75 years old underwent prostate biopsies, irrespective of their PSA levels [4]. Various nomograms and risk assessment tools have been developed to identify men with prostate cancer who have a higher risk of disease progression and mortality. The most commonly used tools include D'Amico risk stratification, CAPRA score, Kattan nomogram and Partin tables [5-8]. A patient's Gleason grade is an important consideration in each of these tools.

A patient's Gleason grade is determined by the pathologist based on the level of glandular differentiation seen in the H&E stained biopsy. A primary and secondary Gleason grade (1-5) is assigned based on the amount of biopsy area containing a particular pattern. The Gleason grades are added up to assign a Gleason score (1-10). The Gleason grade is

Quantitative Phase Imaging, edited by Gabriel Popescu, YongKeun Park, Proc. of SPIE Vol. 9336, 93361U · © 2015 SPIE · CCC code: 1605-7422/15/$18 · doi: 10.1117/12.2080067

considered to be an indicator of possible tumor size, metastasis and outcome [9-12]. A Gleason score of 6 or less is a common criteria used to adopt active surveillance as a prostate cancer management strategy [13]. Thus it's critical to ensure that the Gleason grade is correctly determined. The qualitative nature of Gleason grading can lead to a high degree of disagreements among various pathologists' diagnoses. A study by Allsbrook et. al. showed that the level of under-grading of Gleason score 7 prostate cancer was 47% and that for Gleason score 8-10 prostate cancers was 25% among general pathologists [14]. When the same study was repeated on urologic pathologists, the agreement rate was 70% or higher in the Gl[15]eason score ranges of 2-4, 5-6, 7, 8-10 among the 38 consensus cases but there were 10 non-consensus cases [16]. Clearly, a quantitative technique that can objectively predict Gleason grades with a high degree of accuracy would assist pathologists in performing Gleason grading. This would also have important implications on prostate cancer treatment.

Quantitative phase imaging (QPI) [17]of unstained tissue provides information on the refractive index distribution, or tissue morphology, with nanometer level sensitivity. Subtle morphological changes in both the epithelial and stromal regions of tissue, which are not visible in stained tissue sections used in current pathological settings, can be measured using QPI[15,18-25]Thus QPI would be a valuable addition to current diagnostic pathology. In this paper, we show the ability of QPI to help pathologists quantitatively and therefore, objectively differentiate between Gleason grade 3 and 4 prostate cancers.

2. EXPERIMENTAL DETAILS

2.1 TMA Cohort for the Gleason Grading Study

The tissue microarray (TMA) set used for the Gleason grading study was obtained from the National Cancer Institute Cooperative Prostate Cancer Tissue Resource (NCI-CPCTR). The tissue was collected at four academic institutions: George Washington University, New York University, University of Pittsburg, and Medical College of Wisconsin. Procedures, policies and protocols for TMA construction and slide preparation are available at the CPCTR website [26,27]. The Gleason TMA set includes prostatectomy tissue from 250 patients and includes controls from 18 benign hyperplasia cases. It also includes information on the patient's final Gleason grade diagnosis. The tissue was arrayed into 4 blocks and two 4μm sections were cut. One was deparaffinized and stained with H&E for pathology control. The adjacent section was deparaffinized and coverslipped without staining for SLIM imaging. The studies have been performed in the United States in accordance with the procedure approved by the Institutional Review Board at University of Illinois at Urbana-Champaign (IRB Protocol Number: 13900).

2.2 SLIM Imaging System

Spatial Light Interference Microscopy (SLIM) is a quantitative phase imaging system that was developed as an add-on module to a commercial phase contrast microscope and is described in detail in Ref. [15]. Briefly, the back focal plane of the phase contrast objective is projected onto a liquid crystal phase modulator (LCPM). At the LCPM, three π/2 phase shifts, additional to the one already present in the phase contrast image, are introduced and recorded by the CCD. The four intensity images corresponding to each phase shift are recorded, and a final phase image is computed from the information. The final phase image computed corresponds to:

$$\phi(x,y) = \frac{2\pi}{\lambda} \int_0^{h(x,y)} [n(x,y,z) - n_0]\, dz$$

Where ϕ(x,y) is the phase at a given point, λ is the center wavelength of the white light source (552.3nm), n(x,y,z) is the refractive index at a given point and n_0 is the refractive index of the surrounding medium. The refractive index difference is integrated over the entire thickness of the sample to measure the phase. SLIM has a transverse resolution of 0.4 microns and a spatial path length sensitivity of 0.3nm.

The SLIM system was modified to raster scan through large fields of view and stitch the frames together. This provides the high throughput necessary for whole slide imaging. The samples used in this study were imaged using the 40X/0.75NA objective of the SLIM system.

2.3 Optical Anisotropy

Optical anisotropy is defined as the average cosine of the scattering angle associated with a single scattering event. Since QPI records both the amplitude and the phase of the light passing through the sample, it has the ability to measure light scattering parameters. Using the scattering phase theorem, the optical anisotropy of light passing through the tissue can be measured as [28]

$$g = 1 - \frac{1}{2k_0^2}\frac{\langle|\nabla[\varphi(r)]|^2\rangle_r}{\langle\Delta\varphi^2(r)\rangle_r^2}$$

Where k0 is the wave number of the light source, $\nabla[\varphi(r)]$ is the phase gradient and $\Delta\varphi^2(r)$ is the variance of the phase. The phase gradient and phase variance are averaged over a tissue region of interest, r. In our study, the region of interest was a single layer of stroma immediately adjoining the glands, as shown in Fig. 1.

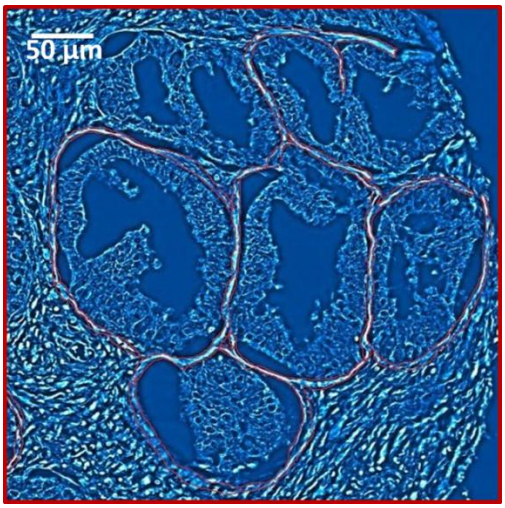

Figure 1: Stromal Region Selection. A single layer of stroma immediately adjoining these glands is highlighted in red in the above image. We calculate optical anisotropy in this layer of stroma using the scattering phase theorem.

2.4 Solidity

Glandular solidity is defined the ratio of the area of the gland to that of the area of a convex hull fit around the gland (Fig. 2). This parameter is an indicator of the uniformity of the edges of the selected tissue region. In order to measure glandular solidity, the glands of interest were selected using the ROI feature on ImageJ. ImageJ was then used to measure the area of the gland, fit a convex hull around the gland, measurement of the area of the convex hull and finally, the solidity.

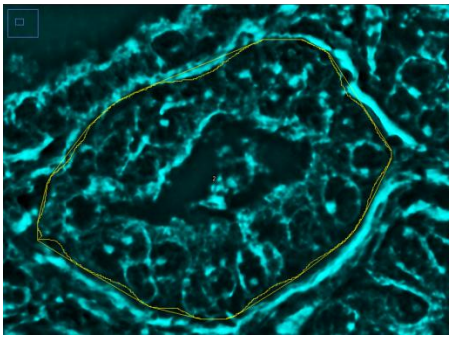

Figure 2: Glandular Solidity. Solidity is defined as the ratio of the area of the gland to the area of the convex hull or polygonal fit around the gland. In the above image, the inner boundary is the ROI of the gland, and the outer boundary shows the convex hull around the gland.

3. RESULTS

43 cases from the TMA 2 data set with consensus diagnosis from 3 pathologists were analyzed. 22 cores with only Gleason grade 3 glands from patients with a final diagnosis of Gleason 3+3 cancer and 21 cores with only Gleason 4 glands and final diagnosis of Gleason 4+4 cancer were imaged using SLIM. Solidity, which the ratio of the area of the gland to that of a convex hull fit around the gland, was measured for all glands in the cores. Additionally, anisotropy, which is the average cosine of the scattering angle, was measured for the layer of stroma surrounding all the glands. Our study showed that Gleason 3 glands had a higher degree of solidity and higher values of anisotropy in the stroma immediately adjoining the gland (Fig. 3). Using glandular solidity and stromal anisotropy alone, 81% of the Gleason grade 4 cores and 82% of the Gleason grade 3 cores were correctly classified. We believe the higher glandular solidity values can be explained by the reduced invasive edges and lower degree of glandular fusion seen in Gleason 3 glands. Additionally, the lower value of anisotropy seen around Gleason grade 4 glands means the stromal layer has a higher level of disorder in advanced stages of disease.

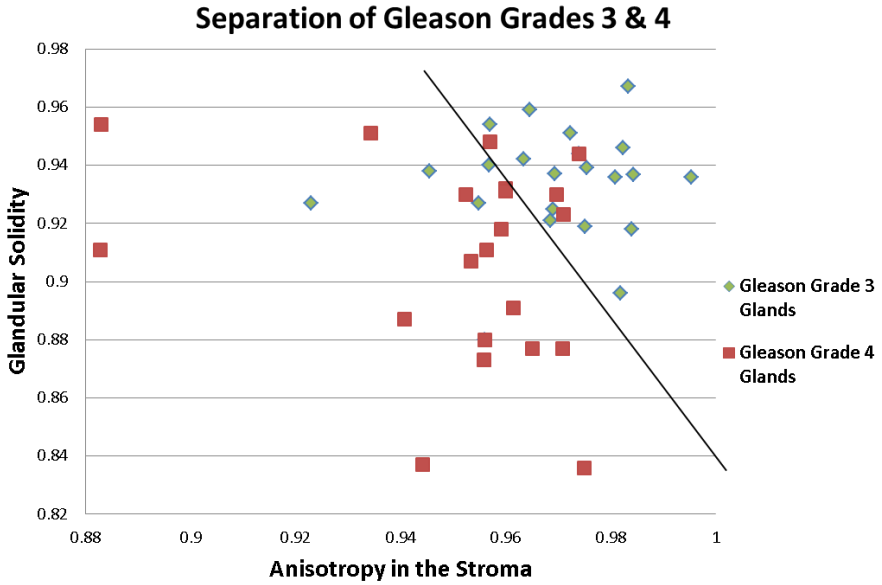

Figure 3 Diagnosis of Gleason Grades 3 and 4 Gleason grade 3 glands have a higher degree of solidity and the stroma surrounding Gleason grade 3 glands have a higher value of anisotropy. Glandular solidity and stromal anisotropy can be used to identify Gleason grade 3 glands with 82% accuracy and Gleason grade 4 glands with 81% accuracy.

4. CONCLUSION AND FUTURE WORK

QPI was able to distinguish between the Gleason grade 3 and 4 prostate cancers with an accuracy of 81.39%. QPI can thus be used to assist pathologists with Gleason grading, especially in difficult cases. Further studies need to be conducted on biopsies to determine if the parameters measured using QPI can be used to predict disease progression with a higher degree of accuracy than existing methods.

5. ACKNOWLEDGEMENTS

This work was supported by the National Science Foundation CBET-1040461 MRI and Agilent Laboratories. For more information, visit www.light.ece.illinois.edu. We thank Jon Liang, Ryan Tapping, Abhijit Marar, Le Wang, Mike Xiang and Karan Shah for the help they provided with image processing.

REFERENCES

[1] N. A. Howlader N, Krapcho M, Garshell J, Miller D, Altekruse SF, Kosary CL, Yu M, Ruhl J, Tatalovich Z,Mariotto A, Lewis DR, Chen HS, Feuer EJ, Cronin KA, [SEER Cancer Statistics Review, 1975-2011] National Cancer Institute. Bethesda, MD, (2014).

[2] A. Bill-Axelson, L. Holmberg, H. Garmo *et al.*, "Radical Prostatectomy or Watchful Waiting in Early Prostate Cancer," New England Journal of Medicine, 370(10), 932-942 (2014).

[3] T. J. Wilt, M. K. Brawer, K. M. Jones *et al.*, "Radical Prostatectomy versus Observation for Localized Prostate Cancer," New England Journal of Medicine, 367(3), 203-213 (2012).

[4] M. P. Porter, J. L. Stanford, and P. H. Lange, "The distribution of serum prostate-specific antigen levels among American men: Implications for prostate cancer prevalence and screening," Prostate, 66(10), 1044-1051 (2006).

[5] A. W. Partin, L. A. Mangold, D. M. Lamm *et al.*, "Contemporary update of prostate cancer staging nomograms (Partin tables) for the new millennium," Journal of Urology, 168(1), 374-375 (2002).

[6] M. W. Kattan, J. A. Eastham, A. M. F. Stapleton *et al.*, "A preoperative nomogram for disease recurrence following radical prostatectomy for prostate cancer," Journal of the National Cancer Institute, 90(10), 766-771 (1998).

[7] A. V. D'Amico, R. Whittington, S. B. Malkowicz *et al.*, "Biochemical outcome after radical prostatectomy, external beam radiation therapy or interstitial radiation therapy for clinically localized prostate cancer," Renal, Bladder, Prostate and Testicular Cancer: An Update, 147-157 (2001).

[8] M. R. Cooperberg, D. J. Pasta, E. P. Elkin *et al.*, "The University of California, San Francisco cancer of the prostate risk assessment score: A straightforward and reliable preoperative predictor of disease recurrence after radical prostatectomy," Journal of Urology, 173(6), 1938-1942 (2005).

[9] P. A. Humphrey, "Gleason grading and prognostic factors in carcinoma of the prostate," Mod Pathol, 17(3), 292-306 (2004).

[10] J. I. Epstein, A. W. Partin, J. Sauvageot *et al.*, "Prediction of progression following radical prostatectomy. A multivariate analysis of 721 men with long-term follow-up," Am J Surg Pathol, 20(3), 286-92 (1996).

[11] A. W. Partin, M. W. Kattan, E. N. Subong *et al.*, "Combination of prostate-specific antigen, clinical stage, and Gleason score to predict pathological stage of localized prostate cancer. A multi-institutional update," JAMA, 277(18), 1445-51 (1997).

[12] L. Egevad, T. Granfors, L. Karlberg *et al.*, "Prognostic value of the Gleason score in prostate cancer," BJU Int, 89(6), 538-42 (2002).

[13] M. A. Dall'Era, M. R. Cooperberg, J. M. Chan *et al.*, "Active surveillance for early-stage prostate cancer," Cancer, 112(8), 1650-1659 (2008).

[14] W. C. Allsbrook, Jr., K. A. Mangold, M. H. Johnson *et al.*, "Interobserver reproducibility of Gleason grading of prostatic carcinoma: general pathologist," Hum Pathol, 32(1), 81-8 (2001).

[15] Z. Wang, L. J. Millet, M. Mir *et al.*, "Spatial light interference microscopy (SLIM)," Optics Express, 19(2), 1016 (2011).

[16] W. C. Allsbrook, Jr., K. A. Mangold, M. H. Johnson *et al.*, "Interobserver reproducibility of Gleason grading of prostatic carcinoma: urologic pathologists," Hum Pathol, 32(1), 74-80 (2001).

[17] G. Popescu, [Quantitative phase imaging of cells and tissues] McGraw-Hill, New York(2011).

[18] G. Popescu, T. Ikeda, R. R. Dasari *et al.*, "Diffraction phase microscopy for quantifying cell structure and dynamics," Optics Letters, 31(6), 775-777 (2006).

[19] C. Edwards, B. Bhaduri, B. G. Griffin *et al.*, "Epi-illumination diffraction phase microscopy with white light," Optics Letters, 39(21), 6162-6165 (2014).

[20] T. Ikeda, G. Popescu, R. R. Dasari *et al.*, "Hilbert phase microscopy for investigating fast dynamics in transparent systems," Optics Letters, 30(10), 1165-1167 (2005).

[21] T. Kim, R. Zhou, M. Mir *et al.*, "White-light diffraction tomography of unlabeled live cells," Nat Photon, 8, (2014).

[22] Y. K. Park, G. Popescu, K. Badizadegan *et al.*, "Diffraction phase and fluorescence microscopy," Optics Express, 14(18), 8263-8268 (2006).

[23] D. Boss, J. Kuehn, C. Depeursinge *et al.*, "Quantitative Measurement of absolute cell volume and intracellular integral refractive index (RI) with Dual-wavelength Digital Holographic Microscopy (DHM)," Biophotonics: Photonic Solutions for Better Health Care Iii, 8427, (2012).
[24] K. J. Chalut, W. J. Brown, and A. Wax, "Quantitative phase microscopy with asynchronous digital holography," Optics Express, 15(6), 3047-3052 (2007).
[25] P. Ferraro, D. Alferi, S. De Nicola *et al.*, "Quantitative phase-contrast microscopy by a lateral shear approach to digital holographic image reconstruction," Optics Letters, 31(10), 1405-1407 (2006).
[26] J. J. Berman, M. Datta, A. Kajdacsy-Balla *et al.*, "The tissue microarray data exchange specification: implementation by the Cooperative Prostate Cancer Tissue Resource," BMC Bioinformatics, 5, 19 (2004).
[27] A. Kajdacsy-Balla, J. M. Geynisman, V. Macias *et al.*, "Practical aspects of planning, building, and interpreting tissue microarrays: the Cooperative Prostate Cancer Tissue Resource experience," J Mol Histol, 38(2), 113-21 (2007).
[28] Z. Wang, H. Ding, and G. Popescu, "Scattering-phase theorem," Optics Letters, 36, 1215 (2011).